

Critical nonequilibrium cluster-flip relaxations in Ising models

Yusuke Tomita

College of Engineering, Shibaura Institute of Technology, Saitama, Saitama 337-8570, Japan

Yoshihiko Nonomura

International Center for Materials Nanoarchitectonics, National Institute for Materials Science, Tsukuba, Ibaraki 305-0044, Japan

(Received 20 August 2018; published 12 November 2018)

We investigate nonequilibrium relaxations of Ising models at the critical point by using a cluster update. While preceding studies imply that nonequilibrium cluster-flip dynamics at the critical point are universally described by the stretched-exponential function, we find that the dynamics changes from the stretched exponential to the power function as the dimensionality is increased: The two-, three-, four-, and infinite-dimensional Ising models are numerically studied, and the four- and infinite-dimensional Ising models exhibit the power-law relaxation. We also show that the finite-size scaling analysis using the normalized correlation length is markedly effective for the analysis of relaxational processes rather than the direct use of the Monte Carlo step.

DOI: [10.1103/PhysRevE.98.052110](https://doi.org/10.1103/PhysRevE.98.052110)**I. INTRODUCTION**

Studies of relaxational processes do not merely give insights but also give probes to investigate critical phenomena. The droplet theory [1,2] gives relations between relaxational processes and droplet excitations, and these enable us to study droplet structures by observing relaxations of order parameters [3]. The nonequilibrium relaxation (NER) method gives us an alternative means to investigate critical phenomena [4]. The NER functions show power-law relaxations at a critical point, whereas they are exponential at off-critical points. The powers of the power functions consist of critical and dynamical exponents. The NER method estimates a critical point by finding a point where relaxations exhibit power-law relaxations, and critical exponents are estimated by applying a scaling ansatz to the power-law relaxation functions. While the NER method examines relaxational processes of sudden cooling and/or heating, a method using the Kibble-Zurek scaling ansatz examines relaxational processes of scheduled cooling and/or heating [5–9]. The way of using scheduled temperature-changing protocol enables us to study a variety of nonequilibrium relaxations in spin systems.

Although examining dynamical quantities rather than static ones is an indirect approach, it is effective for systems whose relaxations are slow. Methods utilizing general relations in the nonequilibrium relaxation do not require thermalization; all the production runs are started without discarding Monte Carlo steps for thermalization.

Since cluster-flip update algorithms [10,11] significantly accelerate Monte Carlo simulation, the algorithms are widely used especially for extensive simulations [12]. The algorithms unite correlated spins into a cluster and flip clusters at a time. The global update reduces autocorrelation time and enables us to sample evenly in a state space with small Monte Carlo steps.

One of us has proposed a method which integrates the NER method and the cluster-flip update [13]. In that study, it was found that the nonequilibrium relaxation of the Ising model at the critical point is not described by the power law, which

is expected in the NER method with single-spin-flip updates, but rather by the stretched-exponential relaxations [13]. Our follow-up studies have revealed that stretched-exponential relaxations are common in the NER with the cluster-flip update [14,15].

To further develop the method which integrates the NER method and cluster-flip update, an understanding of the origin of the stretched-exponential relaxation is indispensable. In this paper, critical nonequilibrium relaxations with cluster update in two-, three-, four-, and infinite-dimensional Ising models are examined. Through the systematical change in the dimensionality, the origin of the stretched-exponential relaxation is investigated.

This paper is organized as follows. In Sec. II the Hamiltonian and the numerical method used in the paper are given. Results for several dimensional Ising models are given in Sec. III. The analysis used in the paper can be extended to a general procedure for investigation of critical phenomena, and the procedure is summarized in Sec. IV. Section V is devoted to summary and discussion.

II. MODEL AND METHOD

We investigate the NER at critical points for two-, three-, four-, and infinite-dimensional Ising models. The Hamiltonian of the finite-dimensional Ising model is given by

$$\mathcal{H} = -J \sum_{(i,j)} \sigma_i \sigma_j, \quad (1)$$

where J is the exchange coupling constant, $\sigma_i \in \{\pm 1\}$ is an Ising spin at site i , and the sum runs over nearest neighbors. On the other hand, the Hamiltonian of the infinite-range Ising model is given by

$$\mathcal{H} = -\frac{J}{N} \sum_{i < j} \sigma_i \sigma_j, \quad (2)$$

where N is the number of sites. The normalization factor N is required to make the system extensive. Hereafter, the Boltzmann constant and the exchange coupling constant J are set to unity.

In the present paper, we observe NERs from totally random states ($T = \infty$) to critical states ($T = T_c$) in the Ising models using the cluster update. To update the systems uniformly, we employ the Swendsen-Wang (multiple) cluster update [10,16,17]. The Wolff (single) cluster update [11] tends to flip larger clusters, and it could bring about spatially nonuniform updates especially in the initial stage.

The computational cost of the Swendsen-Wang cluster algorithm for the infinite-range model is $O(N^2)$ since it scans all the N^2 bonds. To reduce the cost to $O(N)$, the $O(N)$ cluster Monte Carlo method [18–20] is employed. The method skips the bond scan properly and realizes $O(N)$ computational cost.

III. RESULTS

A. Infinite-range Ising model

To understand the NER in the cluster-flip update, we consider time evolution in the infinite-range (IR) Ising model first since the model is one of the simplest models which exhibits phase transitions at a finite temperature. The IR Ising model is an Ising model on the complete graph. Owing to the special character of the complete graph, the development of the magnetization from the completely random configuration ($T = \infty$) to the critical state can be described by the simple exponential form (see Appendix B). We refine the exponential form [Eq. (B12)] by considering three facts: (i) The absolute magnetization per site converges to its thermal equilibrium states $\langle |m_c| \rangle$ [18,19], which is given by Eq. (A13),

$$N^{1/4} \langle |m_c| \rangle = \frac{12^{1/4} \Gamma(1/2)}{\Gamma(1/4)}, \quad (3)$$

$$\sim 0.909890588,$$

where $\Gamma(x)$ is the gamma function. (ii) The first step of the time evolution is the percolation process on the complete graph at the critical point, and the magnetization is proportional to $N^{\beta_p/d_p \nu_p}$, where $\beta_p (= 1)$ and $\nu_p (= 1/2)$ are, respectively, the mean-field critical exponents of the percolation problem for the spontaneous magnetization and the correlation length. The upper critical dimension of the percolation problem d_p is six. (iii) The time scale per one Monte Carlo step depends on the system size. The growth rate of the correlation in the cluster-flip update is proportional to the correlation length ξ and merging rate $S(t)$, and it is described by

$$\frac{d\xi}{dt} = S(t)\xi. \quad (4)$$

Owing to the peculiarity of the complete graph, the merging rate $S(t)$ at the criticality is proportional to the number of outside sites of ordered domains times the density of bonds,

$$S(t) = A \frac{M_\infty - M(t)}{N}, \quad (5)$$

where M_∞ , $M(t)$, and A are, respectively, the magnetization at the thermodynamic limit, the magnetization at Monte

Carlo step t , and a constant. Considering that $M \propto N^{3/4}$ (see Appendix A), Eq. (4) gives that the time scale of the IR Ising model is proportional to $N^{-1/4}$. Taking account of facts (i)–(iii), the scaling function form of the absolute magnetization per site at Monte Carlo step t is refined as

$$\langle |m(t)| \rangle = \langle |m_c| \rangle [1 - \{1 - c_1(t/N^{1/4})^{2/3}\} \times \exp(-c_2 t/N^{1/4})]^{1/2}. \quad (6)$$

Here, c_1 and c_2 are coefficients.

Monte Carlo simulations of the IR Ising model with the $O(N)$ cluster Monte Carlo method [18–20] are executed to obtain the numerical data. To obtain sample means, 8×10^5 independent runs are executed for each system size, $N = 1024, 2048, 4096, 8192, \text{ and } 16384$. Figure 1(a) shows magnetizations per site as functions of Monte Carlo step t for several system sizes, and the finite-size scaling (FSS) plot is shown in Figs. 1(b) and 1(c). The constants c_1 and c_2 in Eq. (6) are 0.463(2) and 0.627(2), respectively. The number in parenthesis represents one standard error in the last digit. The finite-size scaling function is well described by a single curve, and that confirms that in the IR Ising model with Swendsen-Wang cluster updates, the magnetization relaxes toward its equilibrium value according to a product of power and simple exponential functions. At the very beginning of the nonequilibrium relaxation, the magnetization shows the power-law relaxation, and it exponentially converges to the thermal equilibrium value [see Fig. 1(c)]. Finite-size scaling collapse occurs when the Monte Carlo step number t is scaled by $N^{1/4}$; that is, the dynamical exponent is unity since the effective dimension of the model is four.

B. Finite-dimensional Ising model

In our previous papers, we observed stretched-exponential relaxations in the cluster-flip NER at critical points [13–15]. The observation of the stretched-exponential relaxation indicates that the cluster-flip NER is essentially faster than the power-law relaxation which is usually observed in the single-spin-flip NER. The essential difference comes from growing processes in ordering. While most spin updates take place on boundaries of domains of the order parameter in the single-spin-flip update, domains of the order parameter merge into larger domains in the cluster-flip update. This indicates, as explained in the previous section [see Eq. (4)], the relaxational time in the cluster-flip update is proportional to the correlation length. The nonequilibrium relaxation process in the finite-dimensional ($d = 2, 3, \text{ and } 4$) Ising model can be different from the IR Ising model. In an ideal situation like the IR Ising model, a major cluster merges immediate clusters at each Monte Carlo step, and the correlation length develops ballistically ($\xi \propto t$). In the finite-dimensional model, however, a growth rate of clusters fluctuates from place to place, and the relative size of clusters surrounding a major cluster tends to be smaller as the system evolves. If we assume that the merging rate in Eq. (4) is

$$S(t) = ct^{\sigma-1} \quad (\sigma < 1), \quad (7)$$

we obtain

$$\xi(t) = c \exp[(t/\tau)^\sigma], \quad (8)$$

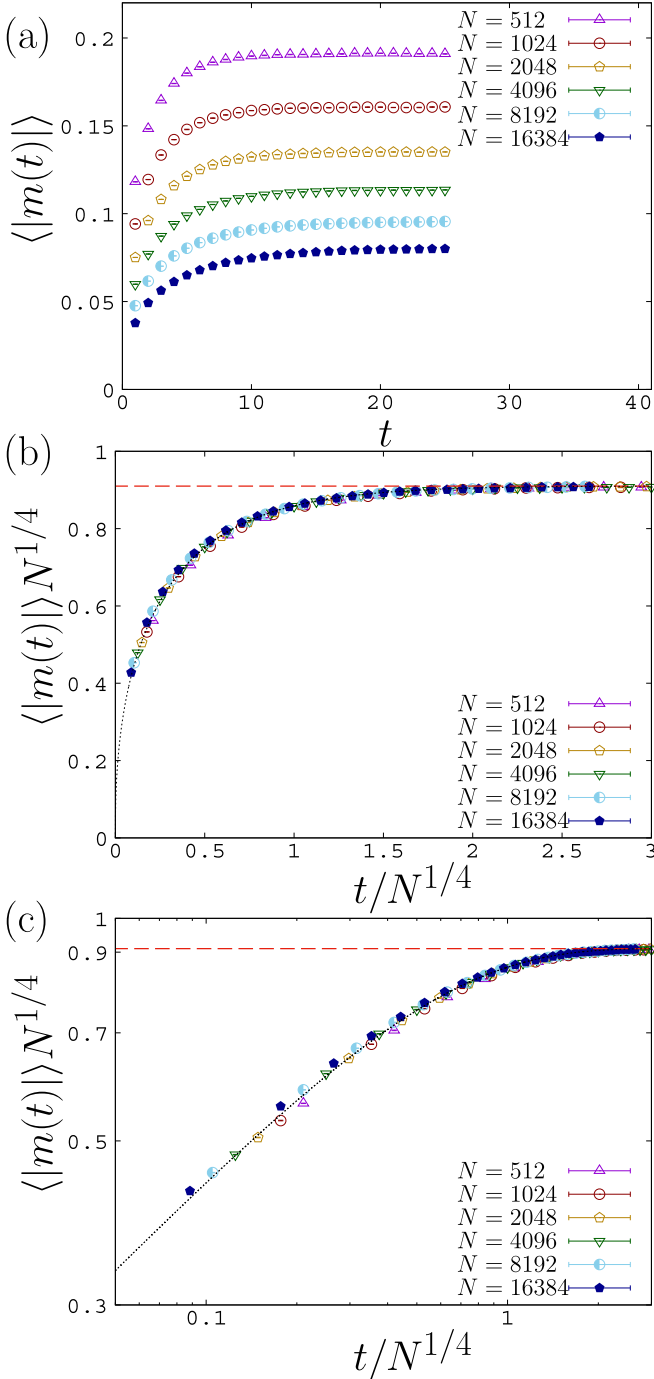


FIG. 1. (a) Magnetizations per site of IR Ising model as functions of Monte Carlo step t for several system sizes. (b) Scaling plot of the magnetization per site of IR Ising model in a linear scale and (c) the same plot in a logarithmic scale. The curve shows the fitting result of Eq. (6). The red broken line indicates the thermodynamic limit value, $12^{1/4}\Gamma(1/2)/\Gamma(1/4)$. Error bars are smaller than the size of the symbols.

where c and τ are constants. The stretched-exponential relaxation conforms to our previous results [13–15].

To examine the stretched-exponential development of the correlation length, we estimate the correlation length as a function of Monte Carlo step t , $\xi(t)$, by the two-point

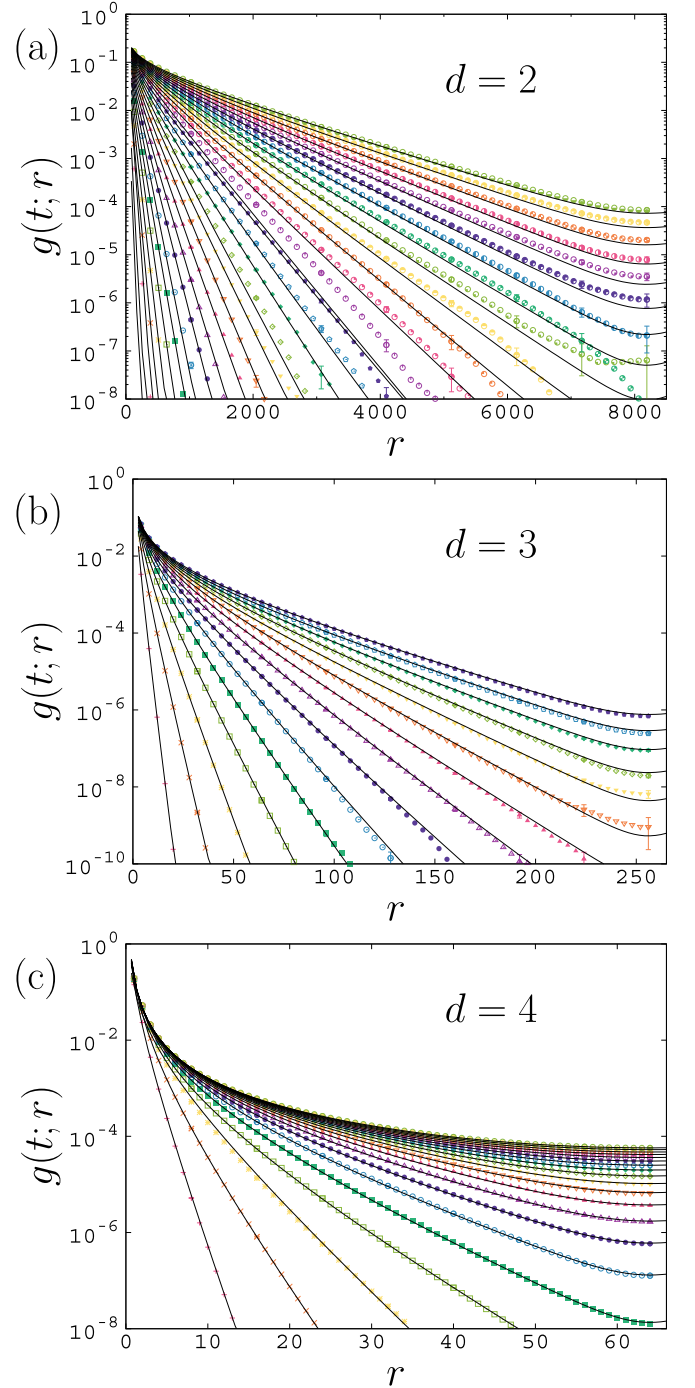


FIG. 2. Two-point function for (a) the two-, (b) three-, and (c) four-dimensional Ising models. Curves show the fitting results of Eq. (11). Slopes are proportional to the inverse of correlation length. As the correlation length develops with time, slopes of curves change from steep to gentle. To avoid impairing the visibility of figures, error bars are plotted for every eighth data point.

correlation function. The time-dependent two-point correlation function is given by

$$g(t; r) = \langle \sigma(t; r_0) \sigma(t; r_0 + r) \rangle, \quad (9)$$

where $\sigma(t; r)$ is the Ising spin variable at time t and position r . To estimate the two-point function effectively, an improved

estimator is used,

$$g(t; r_i, r_j) = \langle \delta(t; r_i, r_j) \rangle, \quad (10)$$

where $\delta(t; r_i, r_j)$ is unity if sites at r_i and r_j belong to the same cluster at time t and is zero otherwise. The angle brackets $\langle \dots \rangle$ denote a sample average. We estimate the correlation length by assuming the functional form of the two-point function as

$$g(t; r) = A \left(\frac{e^{-r/\xi(t)}}{r^{d-2+\eta}} + \frac{e^{-(L-r)/\xi(t)}}{(L-r)^{d-2+\eta}} \right), \quad (11)$$

where r , L , η , d , and A are, respectively, a spatial distance between two spins, a system size, the critical exponent of the correlation function, the spatial dimension, and a constant [21]. The function form is symmetrized, taking account of periodic boundary conditions, which are imposed on our Monte Carlo simulations. Figure 2 shows the two-point functions for the two-, three-, and four-dimensional Ising model. For the two-dimensional model, the temperature is set to the critical temperature, $T_c = 2/\ln(1 + \sqrt{2})$. For the three- and four-dimensional models, critical temperatures are estimated by durations to reach equilibrium states in NER, and they are, respectively, 4.511525 for $d = 3$ and 6.680400 for $d = 4$. The temperatures are given in Table I. Although more precise estimations for the $d = 3$ [22] and 4 [23] Ising models are available, we set the critical temperatures to those estimated by NER. Our estimated temperatures are accurate enough for the study of the cluster-flip NER [24], so the differences in the estimated critical temperatures do not affect critical cluster-flip NER. To obtain sample means, 10^4 independent runs are executed for each system size.

The correlation lengths estimated from the two-point functions for the two-, three-, and four-dimensional Ising models are plotted in insets of Fig. 3. To examine the development of the correlation length, we assume the following form for the stretched-exponential relaxation:

$$\xi(t) = A \exp(t^\sigma / \rho), \quad (12)$$

where A , ρ , and σ are constants. Since the dimension of the correlation length is L , we obtain a dimensionless parameter by dividing the correlation length by the system size L ,

$$\xi(t)/L = A \exp[(t^\sigma - \rho \ln L)/\rho]. \quad (13)$$

The normalized correlation length gives a system-size-independent measure of ordering. The normalized correlation length as a function of t [Eq. (13)] indicates the

TABLE I. Parameters used for our simulations. While the critical temperatures T_c are exact for the $d = 2$ and ∞ (the IR Ising model), those for the $d = 3$ and 4 are estimated by the nonequilibrium relation method. The exact critical exponents β/ν are used for the $d = 2$ Ising model. For the $d = 4$ and ∞ models, the mean-field values are used. For the $d = 3$ model, the values estimated in Ref. [25] are used.

d	T_c	β/ν
2	$2/\ln(1 + \sqrt{2})$	1/8
3	4.511525	0.5181489
4	6.680400	1
∞	1	1

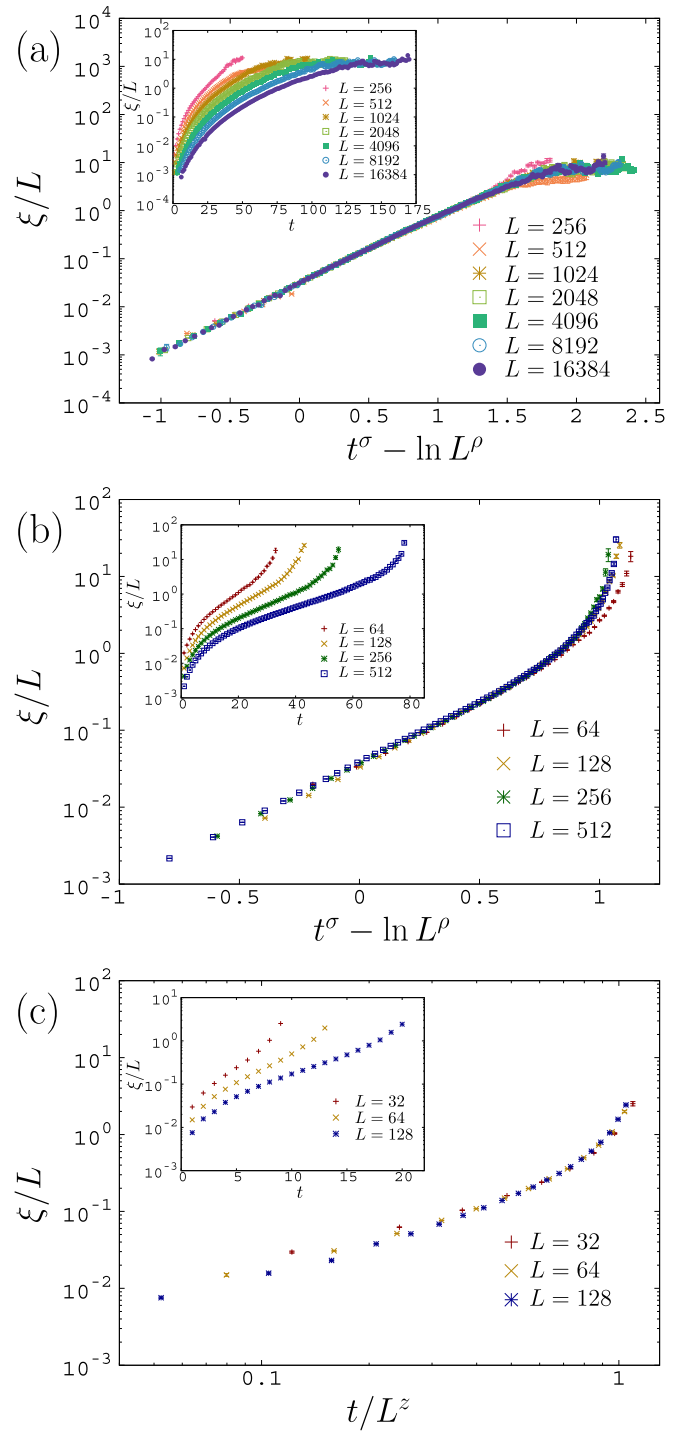


FIG. 3. Scaling plots of normalized correlation lengths for the (a) two-, (b) three-, and (c) four-dimensional Ising models. Insets show the normalized correlation lengths as a function of Monte Carlo step t . Error bars are plotted but are barely visible.

scaling variable of $\xi(t)/L$ is $t^\sigma - \ln L^\rho$, and the two- and three-dimensional data are well scaled by the variable [see Figs. 3(a) and 3(b)]. The parameters for the FSS plot are, respectively, $\sigma = 0.314(2)$ and $\rho = 0.290(4)$ for the two-dimensional model and $\sigma = 0.241(7)$ and $\rho = 0.29(2)$ for the three-dimensional model. While the development of the

correlation length is described by the stretched-exponential function for the two- and three-dimensional Ising models, the FSS scaling plot using Eq. (13) fails for the four-dimensional Ising model. The failure stems from the smallness of the parameter σ . In the limit $\sigma \rightarrow 0$, Eqs. (4) and (7) deduce a power-law relaxation,

$$\xi(t) = At^\alpha, \quad (14)$$

where A and α are constants. The normalized correlation length for the power-law relaxation is given by

$$\xi(t)/L = A(t/L^{1/\alpha})^\alpha, \quad (15)$$

so that the scaling variable is $tL^{-1/\alpha}$. Figure 3(c) shows the finite-size scaling plot of the normalized correlation length for the four-dimensional Ising model. The dynamical exponent $z(= 1/\alpha)$ is estimated as 0.61(1). The upper critical dimension of the Ising model is four, and the power-law form conforms to the result of the IR Ising model. However, the dynamical exponent is smaller than that of the IR Ising model, $z = 1$.

To see that $\xi(t)/L$ is an essential measure of the cluster-flip dynamics, absolute magnetizations per site are plotted as functions of $\xi(t)/L$ in Fig. 4. In the usual FSS scaling for equilibrium states, $(T - T_c)L^{1/\nu}[\propto (L/\xi)^{1/\nu}]$ is used as the scaling variable, and we replace it with $\xi(t)/L$. The modified FSS expression for the absolute magnetization per site is

$$\langle |m(t)| \rangle = L^{-\beta/\nu} \tilde{m}(\xi(t)/L), \quad (16)$$

where \tilde{m} is a scaling function (see Appendix C). In the left-hand side, the thermal average of the absolute value of the magnetization per site is estimated, since the sign of the magnetization frequently flips, accompanying a flip of a major cluster. The exact critical exponents, $\beta = 1/8$ and $\nu = 1$ for the two-dimensional and $\beta = 1/2$ and $\nu = 1/2$ for the four-dimensional Ising model, are used for the scaling plot for the two- and four-dimensional data. For the three-dimensional data, $\beta/\nu = 0.5181489(10)$ is used, which is obtained from the conformal bootstrap with mixed correlators [25]. The critical exponents are given in Table I. At the beginning of the nonequilibrium relaxation, the scaling function \tilde{m} is proportional to the power of $\xi(t)/L$. Solid lines in Fig. 4 are fitting results, and their powers are, respectively, 0.8947(4), 0.9423(7), and 0.901(2) for the two-, three-, and four-dimensional Ising models.

IV. CLUSTER NONEQUILIBRIUM RELAXATION METHOD USING NORMALIZED CORRELATION LENGTH

The analysis of the nonequilibrium relaxation of the correlation length in the present paper shows the FSS analysis using the normalized correlation length $\xi(t)/L$ is markedly effective. Although the FSS analysis using ξ/L has been widely used for the analysis of the thermally equilibrated systems [26–28], it is worthwhile to describe a procedure of the FSS analysis for the nonequilibrium relaxation.

The procedure is as follows: (i) As in the usual FSS analysis of equilibrium simulations, the transition temperature is estimated at first. The correlation length as a function

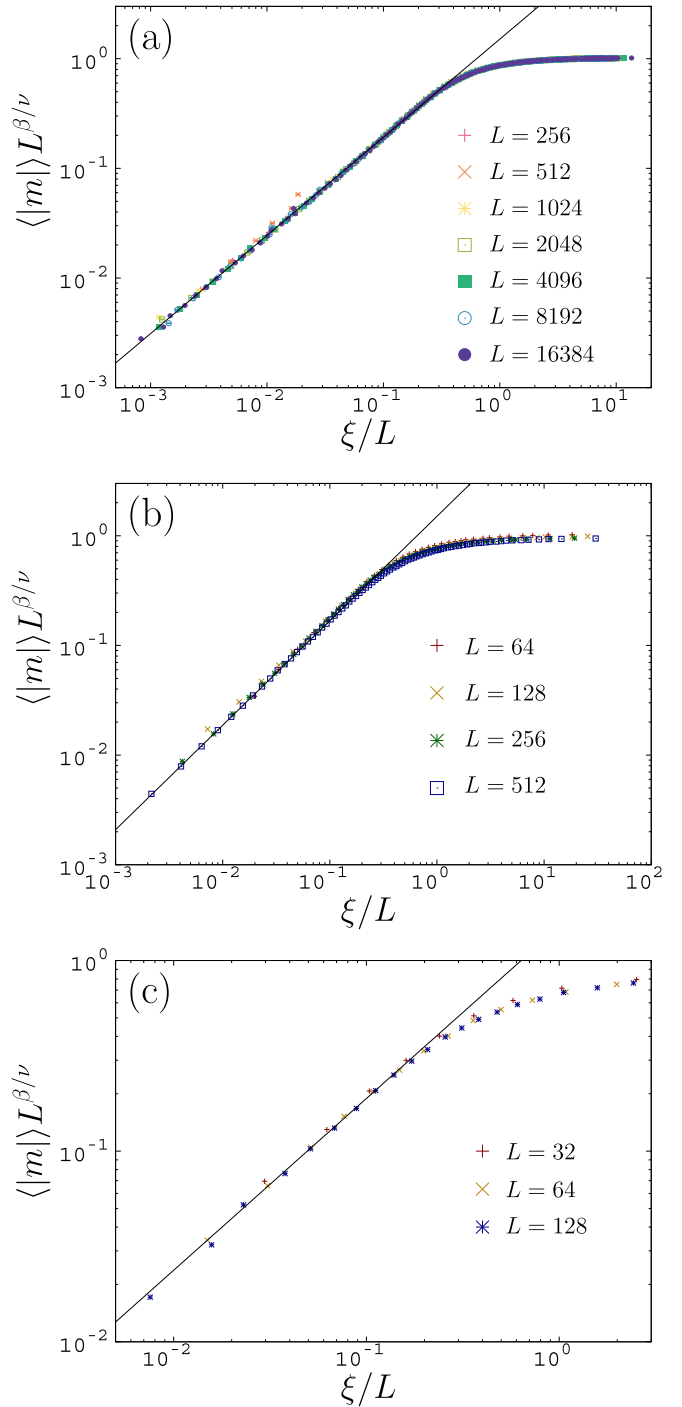


FIG. 4. Finite-size scaling plots of the magnetization for the (a) two-, (b) three-, and (c) four-dimensional Ising models. Lines show fitting results for the scaled magnetizations as functions of the power of $\xi(t)/L$.

of Monte Carlo step t converges to certain values at off critical temperatures, while it constantly develops to the order of the system size at the critical temperature. (ii) After the critical temperature is estimated, critical exponents are estimated by adjusting the vertical scaling factor $L^{\omega/\nu}$ for a quantity in the nonequilibrium relaxation as shown in Fig. 4. Replacing the Monte Carlo step t by the normalized

correlation length $\xi(t)/L$ as the FSS variable, we no longer need to estimate the dynamical exponent z , which is indispensable for the estimation of critical exponents in the NER method [4].

The essence of the method is to describe physical quantities by a dimensionless variable like the normalized correlation length. The normalized correlation length directly reflects correlations of the system, and it helps us to gain insight into relations between physical quantities and the correlation length. In this paper, the normalized correlation length is chosen as the dimensionless variable. However, any dimensionless variables can be used to suit various purposes. For example, the Binder ratio [29] is an alternative dimensionless variable for the cluster NER method [30]. The Binder ratio can be utilized as an indicator of the distribution of order parameter, which takes a trivial value at a trivial fixed point and a nontrivial value at a nontrivial fixed point. Since the Binder ratio is composed of moments of macroscopic order parameters, the analysis using the Binder ratio could be efficient for systems which exhibit a nonuniformly ordered phase.

V. SUMMARY AND DISCUSSION

The nonequilibrium relaxations at the critical points with the cluster update in the Ising models are examined in view of the development of clusters. The analytic form of the nonequilibrium relaxation function of the IR Ising model clarifies that the relaxation is described by the product of the power and simple exponential function. The NER is described by the power-law relaxation at the very beginning, and it shows the simple exponential relaxation just before reaching the thermally equilibrium state. Furthermore, using the peculiarity of the complete graph, it is shown that the system-size dependence of the cluster-flip dynamics is ballistic. These features in the IR Ising model are different from the results observed in the two- and three-dimensional Ising models, in which the relaxation is described by the stretched-exponential form and the system-size dependence of the dynamics is not the usual power law. In the four-dimensional case, which is the upper critical dimension of the Ising model, the system exhibits the power-law relaxation at the very beginning, and the finite-size time scale is proportional to L^z . These features are equivalent to those of the IR Ising model, while the dynamical exponent z is smaller than that of the IR Ising model. This difference in z would come from the finite-size correction. We expect that z is unity in the four-dimensional case since the fluctuation is suppressed enough in the upper critical dimension and the merging rate described in Eq. (5), which deduces $z = 1$, would also be realized in the four-dimensional system. In addition, at the upper critical dimension, the estimation of the critical exponents is difficult because the logarithmic correction severely affects the estimation. There is another possibility that the dynamical exponent depends on the dimensionality and that it converges to unity in the limit of $d \rightarrow \infty$. The examination of the dimensional dependence of the dynamical exponent is left for future studies.

As the finite-size dependence of the time scale depends on the dimensionality, the relaxational dynamics also depends on the dimensionality. While the stretched-exponential relaxation

is observed at $d = 2$ and 3 , the nonequilibrium relaxation is described by the product of the power and simple exponential function at $d = 4$ and $d = \infty$ (the IR Ising model). Therefore, there is a dynamical transition point between $d = 3$ and 4 . Even though they are rough analyses, Eqs. (4) and (7) grasp the mechanism of cluster growth. In the IR Ising model, all the sites reside on the surface of clusters, and the major cluster is able to merge minor clusters at every site. The ease of merging brings about the rapid decrease of minor clusters and of the merging rate. On the other hand, in the finite-dimensional Ising models, only the sites on the surface are able to merge minor clusters. The restriction of the merging process moderates the decrease of the merging rate, and it causes the dynamical transition depending on the dimensionality. The merging rate described in Eq. (7) could be too simplified, but it indicates that the dimensionality of the system and cluster surface contribute to the essential feature of the cluster-flip dynamics. According to the droplet theory [1], it is known that the decay of the temporal autocorrelation function in the ordered phase is stretched-exponential for $d < 3$, while it is simple exponential decay for $d > 3$. Although the cluster-flip dynamics in the nonequilibrium state is different from those dealt with in the droplet theory, our results imply the droplet theory would also be effective for analyzing the cluster-flip dynamics. Further investigation is required to understand the universality class of the cluster-flip dynamics.

A method for investigating critical phenomena with the nonequilibrium cluster-flip update is described in Sec. IV. The applicability of the method is restricted to systems in which the cluster-flip update is effective. However, the method does not require us to equilibrate systems, and an acceleration of relaxation by the cluster-flip update reduces computational time significantly. Combining this method with the Kibble-Zurek scaling ansatz will deepen our understanding of the cluster-flip dynamics.

While relaxational dynamics with the single-spin-flip update are intensively studied, studies of those with the cluster-flip update are not necessarily enough. One reason for its being overlooked is that the cluster-flip update merely seems to be useful but its dynamics are thought to be nonphysical. However, our results show that its dynamics reflect states of systems, and extracting features of systems is possible by analyzing nonequilibrium cluster-flip relaxations. Equilibrium cluster-flip dynamics of the q -state Potts model are studied by analytical [31] and numerical methods [32–35]. Moreover, the cluster-flip dynamics in noninteger q -state Potts models are also investigated [36]. It would be interesting to examine the relation between cluster dynamics and correlation lengths and cluster surfaces [Eq. (4)] in other q -state (including noninteger q) Potts models. There still remains much to be clarified in the cluster-flip dynamics, and further investigations will develop computational methods and deepen an understanding of dynamics in spin systems.

ACKNOWLEDGMENT

This work was supported by JSPS KAKENHI Grant No. 16K05493.

APPENDIX A: MAGNETIZATION OF THE INFINITE-RANGE ISING MODEL NEAR THE CRITICAL POINT

Using the Hubbard-Stratonovich transformation, the partition function of the IR Ising model [Eq. (2)] is given by [37]

$$Z = e^{K/2} \sqrt{\frac{NK}{2\pi}} \int_{-\infty}^{\infty} \exp\{-Ng(K; m)\} dm, \quad (A1)$$

where $g(K; m)$ is

$$g(K; m) = \frac{K}{2} m^2 - \ln(2 \cosh Km). \quad (A2)$$

Here N is the number of sites, and $K (= \beta J)$ is the exchange interaction multiplied by the inverse temperature. Assuming $m \ll 1$, we expand $g(K; m)$ up to the fourth order in m and

obtain

$$g(K; m) \simeq -\ln 2 + \frac{K(1-K)}{2} m^2 + \frac{K^4}{12} m^4. \quad (A3)$$

By replacing $NK^4 m^4$ by $12\mu^2$, the partition function is written as

$$Z = \frac{2^{N-1}(12N)^{1/4}}{\sqrt{2\pi K}} \exp\left(\frac{K}{2} + \frac{3(1-K)^2 N}{4K^2}\right) I, \quad (A4)$$

where I is

$$I = \int_0^{\infty} \mu^{-1/2} \exp\left\{-\left(\mu + \frac{(1-K)\sqrt{3N}}{2K}\right)^2\right\} d\mu. \quad (A5)$$

This integral I is represented by the summation of gamma functions by replacing $(\mu + \sqrt{\epsilon})^2$ by t ,

$$\begin{aligned} I &= \frac{1}{2} \int_{\epsilon}^{\infty} t^{-1/2} (t^{1/2} - \epsilon^{1/2})^{-1/2} e^{-t} dt \\ &= \frac{1}{2} \int_{\epsilon}^{\infty} \sum_{n=0}^{\infty} \frac{(2n-1)!!}{2^n n!} t^{-(2n+3)/4} \epsilon^{n/2} dt \\ &= \frac{1}{2} \sum_{n=0}^{\infty} \frac{(2n-1)!!}{2^n n!} \left\{ \Gamma\left(-\frac{2n-1}{4}\right) - \gamma\left(-\frac{2n-1}{4}, \epsilon\right) \right\} \epsilon^{n/2}, \end{aligned} \quad (A6)$$

where, $\epsilon = 3(1-K)^2 N / (4K^2)$, $\Gamma(a)$ is the gamma function, and $\gamma(a, x)$ is the lower incomplete gamma function. The lower incomplete gamma function has the following asymptotic equation [38]:

$$\gamma(a, x) = \Gamma(a) x^a e^{-x} \sum_{n=0}^{\infty} \frac{x^n}{\Gamma(a+n+1)}. \quad (A7)$$

Using the asymptotic equation, the integral I is rewritten as

$$I = \frac{1}{2} \sum_{n=0}^{\infty} \frac{(2n-1)!!}{2^n n!} \Gamma\left(-\frac{2n-1}{4}\right) \left(\epsilon^{n/2} - \epsilon^{1/4} e^{-\epsilon} \sum_{k=0}^{\infty} \frac{\epsilon^k}{\Gamma((5-2n)/4+k)} \right). \quad (A8)$$

Therefore, the partition function up to the fourth-order in m is given by

$$Z = \frac{2^{N-2}(12N)^{1/4} e^{K/2}}{\sqrt{2\pi K}} \sum_{n=0}^{\infty} \frac{(2n-1)!!}{2^n n!} \Gamma\left(-\frac{2n-1}{4}\right) \left(\epsilon^{n/2} e^{\epsilon} - \epsilon^{1/4} \sum_{k=0}^{\infty} \frac{\epsilon^k}{\Gamma((5-2n)/4+k)} \right). \quad (A9)$$

In a similar manner, the thermal average of the magnetization times the partition function, $\langle |m| \rangle Z$, can be obtained as

$$\begin{aligned} \langle |m| \rangle Z &= 2 e^{K/2} \sqrt{\frac{NK}{2\pi}} \int_0^{\infty} m \exp\{-Ng(K; m)\} dm \\ &= \frac{2^{N-2} \sqrt{12} e^{K/2}}{\sqrt{2\pi K^3}} \Gamma\left(\frac{1}{2}\right) \left(e^{\epsilon} - \epsilon^{1/2} \sum_{k=0}^{\infty} \frac{\epsilon^k}{\Gamma(3/2+k)} \right). \end{aligned} \quad (A10)$$

Combining Eqs. (A9) and (A10), we obtain the magnetization near the critical point as

$$\begin{aligned} \langle |m| \rangle &= \frac{12^{1/4} \Gamma(1/2)}{N^{1/4} K} \left(e^{\epsilon} - \epsilon^{1/2} \sum_{k=0}^{\infty} \frac{\epsilon^k}{\Gamma(3/2+k)} \right) \left\{ \sum_{n=0}^{\infty} \frac{(2n-1)!!}{2^n n!} \Gamma\left(-\frac{2n-1}{4}\right) \right. \\ &\quad \left. \times \left(\epsilon^{n/2} e^{\epsilon} - \epsilon^{1/4} \sum_{k=0}^{\infty} \frac{\epsilon^k}{\Gamma((5-2n)/4+k)} \right) \right\}^{-1}. \end{aligned} \quad (A11)$$

The Taylor series expansion of $\langle |m| \rangle$ with respect to $\epsilon^{1/4}$ is given by

$$\langle |m| \rangle = \frac{12^{1/4}\Gamma(1/2)}{N^{1/4}\Gamma(1/4)K} \left(1 + \sum_{n=1}^{\infty} c_n \epsilon^{n/4} \right), \quad (\text{A12})$$

where c_n is the n th Taylor coefficient. From Eq. (A12), by setting the variables to the critical values $K = 1$ and $\epsilon = 0$, we obtain the value of the absolute magnetization at the critical point,

$$\langle |m_c| \rangle = \frac{12^{1/4}\Gamma(1/2)}{N^{1/4}\Gamma(1/4)}. \quad (\text{A13})$$

APPENDIX B: NONEQUILIBRIUM RELAXATION OF THE MAGNETIZATION IN THE IR ISING MODEL

Using the peculiarity of the complete graph, we derive the development of magnetization of the infinite-range Ising model at the critical point as a function of Monte Carlo step. The magnetization depends on the density of bonds, which are fundamental elements in the graph representation, and we consider the time evolution of the density of bonds rather than the magnetization directly. In the Swendsen-Wang cluster algorithm, we put bonds between parallel spins with the probability p . Denoting the magnetization at the Monte Carlo step $n-1$ by M_{n-1} , the number of spins parallel to the magnetization N_+ and the number of spins antiparallel to the magnetization N_- , respectively, are given by

$$N_+ = \frac{N + M_{n-1}}{2}, \quad (\text{B1})$$

$$N_- = \frac{N - M_{n-1}}{2}. \quad (\text{B2})$$

The number of bonds between parallel spins B_{\parallel} is

$$B_{\parallel} = \frac{N_+(N_+ - 1)}{2} + \frac{N_-(N_- - 1)}{2}. \quad (\text{B3})$$

The probability of a putting bond is

$$p = 1 - e^{-2K/N}. \quad (\text{B4})$$

For large enough N , the probability p near the critical point ($K \sim 1$) is approximately represented as

$$p \simeq \frac{2}{N}. \quad (\text{B5})$$

The density of bonds at Monte Carlo step n , b_n , is given by

$$\begin{aligned} b_n &= \frac{B_{\parallel}}{B}, \\ &= \frac{1}{N} + \frac{1}{N} m_{n-1}^2, \end{aligned} \quad (\text{B6})$$

where B is the number of bonds and m_n is the magnetization per site at Monte Carlo step n . Near the critical point, the magnetization per site m [see Eq. (A12)] is given by

$$m(x) = AN^{-1/4} \left(1 - \sum_{i=1}^{\infty} C_i e^{-3x^4/4} x^i \right), \quad (\text{B7})$$

where A is a constant, C_i is an expansion coefficient, and $x = [(1-K)/K]^{1/2} N^{1/4}$. In the quench process, we assume $x \ll 1$ and $(1-K)/K \propto b_c - b$, where b_c is the density of bonds at the critical point, and b is the density of bonds. Considering the slowest term to converge, Eq. (B6) is rewritten as

$$b_n = \frac{1}{N} + \frac{A_1}{N^{3/2}} \{1 - A_2 N^{3/2} (b_c - b_{n-1})\}, \quad (\text{B8})$$

$$\simeq \frac{1}{N} - A_1 A_2 (b_c - b_{n-1}). \quad (\text{B9})$$

Here, A_1 and A_2 are constants. Solution of this recurrence relation [Eq. (B9)] is given by

$$b_n = b_{\infty} - (b_{\infty} - b_0) r^n, \quad (\text{B10})$$

where $r = A_1 A_2$ and $b_{\infty} = (1/N - r b_c)/(1 - r)$. Combining Eqs. (B10) and (B7), the magnetization at Monte Carlo step n , m_n , is given by

$$m_n \simeq AN^{-1/4} [1 - C \{b_c - b_{\infty} + (b_{\infty} - b_0) r^n\}^{1/2} N^{3/4}]. \quad (\text{B11})$$

In the critical region, the inside of the curly brackets is proportional to $N^{-3/2}$, and we obtain

$$m_n \simeq AN^{-1/4} [1 - c_1 (1 + c_2 e^{-n/\tau})^{1/2}], \quad (\text{B12})$$

where c_1 and c_2 are constants.

APPENDIX C: CRITICAL SCALING OF THE ABSOLUTE MAGNETIZATION

The thermal average of the absolute magnetization $\langle |m(L)| \rangle$ obeys the same finite-size scaling as the spontaneous magnetization. Using the distribution function of the magnetization $P(L; m)$, the absolute magnetization is written as

$$\langle |m(L)| \rangle = \frac{\int_0^{\mu} m P(L; m) dm}{\int_0^{\mu} P(L; m) dm}, \quad (\text{C1})$$

where μ is the upper bound of the magnetic distribution. In the scaling region ($T \sim T_c$), the distribution function is written as

$$P(L; m) = L^{\beta/\nu} \tilde{P}(m L^{\beta/\nu}), \quad (\text{C2})$$

where L is the system size, β is the critical exponent of the order parameter, ν is the critical exponent of the correlation length, and $\tilde{P}(m L^{\beta/\nu})$ is the dimensionless distribution function. By substituting Eq. (C2) into Eq. (C1), we obtain

$$\begin{aligned} \langle |m(L)| \rangle &= \frac{\int_0^{\mu} m L^{\beta/\nu} \tilde{P}(m L^{\beta/\nu}) dm}{\int_0^{\mu} L^{\beta/\nu} \tilde{P}(m L^{\beta/\nu}) dm}, \\ &= L^{-\beta/\nu} \frac{\int_0^{\mu L^{\beta/\nu}} \hat{m} \tilde{P}(\hat{m}) d\hat{m}}{\int_0^{\mu L^{\beta/\nu}} \tilde{P}(\hat{m}) d\hat{m}}, \end{aligned} \quad (\text{C3})$$

where $\hat{m} (= m L^{\beta/\nu})$ is the dimensionless magnetization. In the scaling region, the upper bound μ is proportional to $(T_c - T)^{\beta} \propto \xi^{-\beta/\nu}$, where ξ is the correlation length. The integrals in Eq. (C3), therefore, are written by a function of

the normalized correlation length, $\xi/L(\propto (\mu L^{\beta/\nu})^{-\nu/\beta})$. As a result, Eq. (C3) is written as

$$\langle |m(L)| \rangle = L^{-\beta/\nu} \tilde{m}(\xi/L), \quad (\text{C4})$$

where \tilde{m} is a dimensionless scaling function. Equation (C4) tells us that the absolute magnetization obeys the same finite-size scaling as the spontaneous magnetization.

-
- [1] D. A. Huse and D. S. Fisher, *Phys. Rev. B* **35**, 6841 (1987).
- [2] C. Tang, H. Nakanishi, and J. S. Langer, *Phys. Rev. A* **40**, 995 (1989).
- [3] Y. Tomita, *Phys. Rev. E* **94**, 062142 (2016).
- [4] Y. Ozeki and N. Ito, *J. Phys. A: Math. Theor.* **40**, R149 (2007).
- [5] T. W. B. Kibble, *J. Phys. A: Math. Gen.* **9**, 1387 (1976).
- [6] W. H. Zurek, *Nature* **317**, 505 (1985).
- [7] A. Chandran, A. Erez, S. S. Gubser, and S. L. Sondhi, *Phys. Rev. B* **86**, 064304 (2012).
- [8] C.-W. Liu, A. Polkovnikov, and A. W. Sandvik, *Phys. Rev. B* **89**, 054307 (2014).
- [9] N. Xu, C. Castelnovo, R. G. Melko, C. Chamon, and A. W. Sandvik, *Phys. Rev. B* **97**, 024432 (2018).
- [10] R. H. Swendsen and J.-S. Wang, *Phys. Rev. Lett.* **58**, 86 (1987).
- [11] U. Wolff, *Phys. Rev. Lett.* **62**, 361 (1989).
- [12] Y. Komura and Y. Okabe, *J. Phys. Soc. Jpn.* **81**, 113001 (2012).
- [13] Y. Nonomura, *J. Phys. Soc. Jpn.* **83**, 113001 (2014).
- [14] Y. Nonomura and Y. Tomita, *Phys. Rev. E* **92**, 062121 (2015).
- [15] Y. Nonomura and Y. Tomita, *Phys. Rev. E* **93**, 012101 (2016).
- [16] Y. Komura and Y. Okabe, *Comput. Phys. Commun.* **183**, 1155 (2012).
- [17] Y. Komura, *Comput. Phys. Commun.* **194**, 54 (2015).
- [18] E. Luijten and H. W. Blöte, *Int. J. Mod. Phys. C* **6**, 359 (1995).
- [19] E. Luijten, *Interaction Range, Universality and the Upper Critical Dimension* (Delft University, Delft, 1997).
- [20] K. Fukui and S. Todo, *J. Comput. Phys.* **228**, 2629 (2009).
- [21] We took into account a correction-to-scaling for data of $d = 3$ and $L = 256$. The scaling form we considered is $g(r) = A(\exp(-r/\xi)/[r^{d-2+\eta}(1 + ar^\omega)] + \exp[-(L-r)/\xi]/\{(L-r)^{d-2+\eta}[1 + a(L-r)^\omega]\})$, where ω and a are a correction-to-scaling exponent and a constant, respectively. Fitting of the four-dimensional Ising model data suffers from corrections in small r . To suppress the corrections, for the four-dimensional data, the logarithmic residuals are minimized instead of residuals.
- [22] A. M. Ferrenberg, J. Xu, and D. P. Landau, *Phys. Rev. E* **97**, 043301 (2018).
- [23] P. H. Lundow and K. Markström, *Phys. Rev. E* **80**, 031104 (2009).
- [24] Ratios of the temperatures are 1.0000004 and 1.00002 for the three- and four-dimensional Ising models, respectively.
- [25] F. Kos, D. Poland, D. Simmons-Duffin, and A. Vichi, *J. High Energ. Phys.* **08** (2016) 036.
- [26] S. Caracciolo, R. G. Edwards, S. J. Ferreira, A. Pelissetto, and A. D. Sokal, *Phys. Rev. Lett.* **74**, 2969 (1995).
- [27] S. Caracciolo, R. G. Edwards, A. Pelissetto, and A. D. Sokal, *Phys. Rev. Lett.* **75**, 1891 (1995).
- [28] Y. Tomita, *Phys. Rev. E* **90**, 032109 (2014).
- [29] K. Binder, *Z. Phys. B: Condens. Matter* **43**, 119 (1981).
- [30] Y. Nonomura and Y. Tomita, [arXiv:1801.10315](https://arxiv.org/abs/1801.10315).
- [31] X.-J. Li and A. D. Sokal, *Phys. Rev. Lett.* **63**, 827 (1989).
- [32] J. Salas and A. D. Sokal, *J. Statist. Phys.* **98**, 551 (2000). (Numerical results on equilibrium cluster-flip dynamics are shown in [arXiv:cond-mat/9904038v1](https://arxiv.org/abs/cond-mat/9904038v1).)
- [33] J. Salas and A. D. Sokal, *J. Stat. Phys.* **87**, 1 (1997).
- [34] J. Salas and A. D. Sokal, *J. Stat. Phys.* **88**, 567 (1997).
- [35] G. Ossola and A. D. Sokal, *Nucl. Phys. B* **691**, 259 (2004).
- [36] Y. Deng, T. M. Garoni, J. Machta, G. Ossola, M. Polin, and A. D. Sokal, *Phys. Rev. Lett.* **99**, 055701 (2007).
- [37] H. Nishimori and G. Ortiz, *Elements of phase transitions and critical phenomena*, *Oxford Graduate Texts* (Oxford University, Oxford, 2011).
- [38] M. Abramowitz and I. A. Stegun, *Handbook of Mathematical Functions with Formulas, Graphs, and Mathematical Tables* (Dover, New York, 1964).